

Non-equilibrium dynamics of superconductivity in the Hatsugai-Kohmoto model

Ádám Bácsi^{1,*} and Balázs Dóra^{2,†}

¹*Department of Mathematics and Computational Sciences,
Széchenyi István University, 9026 Győr, Hungary*

²*Department of Theoretical Physics, Budapest University of Technology and Economics, Budapest, Hungary*

(Dated: October 21, 2024)

We study the non-equilibrium dynamics of the superconducting order parameter in the Hatsugai-Kohmoto (HK) model. In the absence of superconductivity, its ground state is a non-Fermi liquid, whose properties are controlled by the HK interaction. Our protocol involves quantum quenching the HK interaction but leaving the interaction responsible for superconductivity unchanged. We map out the non-equilibrium dynamical phase diagram of the interacting model which contains three phases where, at long times, the order parameter amplitude vanishes, approaches a constant value or persistently oscillates. We also investigate the Loschmidt echo in searching for dynamical quantum phase transition, and find no significant correlation between the three phases and the non-analytic temporal behaviour of the Loschmidt echo. The momentum space entanglement entropy between positive and negative momentum modes, relevant for Cooper pairing, is calculated. Counterintuitively, this momentum space entanglement does not change significantly during the quench dynamics and its value remains reasonably large even for vanishing superconducting order parameter. Nevertheless, its derivative with respect to the HK interaction signals the dynamical phase transition associated to the late time vanishing of superconductivity.

I. INTRODUCTION

The investigation of quantum quenches and non-equilibrium dynamics in general represents an important tool in several distinct fields of physics, including condensed matter, cold atoms, high energy physics, mesoscopic systems etc.[1–3]. During the non-equilibrium time evolution, one can on one hand address important and fundamental questions related to equilibration and thermalization, but on the other hand, engineering novel steady states of matter without an equilibrium counterpart is possible, such as e.g. Floquet topological systems without an external drive[4].

This program has been carried out for interacting superconductors upon an abrupt temporal change of the interaction strength, responsible for superconductivity. In general, three different phases are distinguished based on the behaviour of the order parameter in the long time limit: the superconducting order parameter vanishes, approaches a constant value or persistently oscillates [5, 6]. The dynamical phase transition (DPT) between these phases is continuous and occurs as the initial or final interaction is varied[7]. Parallel to these, another notion of dynamical quantum phase transition (DQPT) appeared, which is related to the non-analytic behaviour in time of the Loschmidt echo, namely the overlap of the initial and time evolved wavefunctions[8–10]. For quenched BCS superconductors, the temporal non-analyticity in the Loschmidt echo does not distinguish between distinct dynamical phases[11].

The common feature in these non-equilibrium BCS superconductors is the Fermi-liquid nature of the normal,

non-superconducting ground state. However, recently equilibrium superconductivity[12–18] arising on top of the competition between non-Fermi liquid behaviour and Mottness has been studied in the Hatsugai-Kohmoto (HK) model[19, 20]. Therein, the special structure of the momentum space interaction renders the model exactly solvable and induces non-Fermi liquid behaviour for a wide range of model parameters.

Here we extend previous studies on non-equilibrium interacting BCS superconductivity based on the HK model. In contrast to previous approaches, we study the effect of quantum quenches of the HK interaction on the superconducting order parameter in the initially superconducting HK. We also investigate the conditions for emerging dynamical phase transitions (DPT). We find that for a HK quench, the long time phase diagram has an entirely different structure compared to the conventional case[5, 21–23] with Fermi-liquid normal state, though the ensuing phases display the same three long time behaviours, namely the amplitude of the superconducting order parameter either vanishes or approaches a constant value or persistently oscillates. In particular, we find that by significantly increasing or decreasing the HK interaction during the quench completely suppresses and kills superconductivity in the long time limit, while small changes in the HK interaction result in persistent oscillation of the superconducting order parameter. In between these two extreme regions, the order parameter approaches a constant value[24] through damped oscillations. By investigating the Loschmidt echo, we find no direct correspondence between the non-analyticity of the echo and the order parameter phase diagram.

We also investigated the reduced density matrix of positive momentum modes and the ensuing entanglement entropy between positive and negative momentum modes. We find that it remains sizeable even for vanishing late

* bacsi.adam@sze.hu

† dora.balazs@ttk.bme.hu

time superconducting order parameter. This indicates that although superconductivity is absent from certain final states, superconducting quantum correlations are still relevant.

II. SUPERCONDUCTING HATSUGAI-KOHMOTO MODEL

The HK model [12, 19] is defined by the Hamiltonian

$$H_0 = \sum_k \left(\varepsilon(k)(n_{k\uparrow} + n_{k\downarrow}) + Un_{k\uparrow}n_{k\downarrow} \right) \quad (1)$$

where $n_{k\sigma} = c_{k\sigma}^\dagger c_{k\sigma}$ is the occupation number operator of the electrons with momentum k and spin σ and $\varepsilon(k)$ is the non-interacting band structure. The dimension of the system does not play any qualitative role in the forthcoming calculations and, hence, the dimension of the wavevector k is also not specified. For each momentum k , the Hamiltonian is diagonalizable in the four-dimensional many-body Hilbert space spanned by $|0\rangle$, $|\uparrow\rangle$, $|\downarrow\rangle$ and $|\uparrow\downarrow\rangle$ denoting the states with zero particle, one spin up particle, one spin down particle and two particles, respectively. The eigenvalues are 0 for the empty state, $\varepsilon(k)$ for singly occupied state with either a spin up or a spin down particle, and finally $2\varepsilon(k) + U$ for the doubly occupied case. The band structure is best represented by a lower ($\varepsilon(k)$) and an upper Hubbard band ($\varepsilon(k) + U$) [12]. The two Hubbard bands overlap if $U < W$ and are completely separated for $U \geq W$ where W is the bandwidth of the dispersion $\varepsilon(k)$, i.e., $\varepsilon \in (-W/2, W/2)$. At zero temperature, the bands are filled up to the chemical potential μ . The half filling is ensured by the relation

$$\mu = \frac{U}{2} \quad (2)$$

if the bands obey the symmetry of $\rho(\varepsilon) = \rho(-\varepsilon)$ where ρ is the density of states of the energy levels ε . For half filling, the ground state of the system is a non-Fermi liquid for $U < W$ and the amount of non-Fermi liquidness is controlled by U , while it becomes a Mott insulator for $U > W$ [12].

To study superconductivity in the HK model, we consider an attractive interaction [12, 14, 15] of the form

$$H = H_0 - \frac{g}{N} \sum_{kk'} c_{k\uparrow}^\dagger c_{-k\downarrow}^\dagger c_{-k'\downarrow} c_{k'\uparrow} \quad (3)$$

where g is the pairing strength and N is the number of momentum modes. Within mean-field approximation, we assume that the fluctuations around the expectation value $\Delta = \frac{g}{N} \sum_k \langle c_{-k\downarrow} c_{k\uparrow} \rangle$ are negligible, leading to

$$H_{MF} = H_0 + \frac{N|\Delta|^2}{g} - \sum_k \left(\Delta c_{k\uparrow}^\dagger c_{-k\downarrow}^\dagger + h.c. \right). \quad (4)$$

The pairing interaction connects the sectors corresponding to k and $-k$. The overall many-body Hilbert space

for a given $(k, -k)$ becomes 16-dimensional [15]. In this Hilbert space, all possible occupation configurations of the states $k \uparrow$, $k \downarrow$, $-k \uparrow$ and $-k \downarrow$ are taken into account. By considering the ensuing pseudo-spins [5, 25] of these four states, the direct product of the four spin- $\frac{1}{2}$ space results in the direct sum of a quintet subspace (spin-2), 3 triplet subspaces (spin-1) and 2 singlet subspaces (spin-0) as

$$\mathcal{H}_{\frac{1}{2}} \otimes \mathcal{H}_{\frac{1}{2}} \otimes \mathcal{H}_{\frac{1}{2}} \otimes \mathcal{H}_{\frac{1}{2}} = 2\mathcal{H}_0 \oplus 3\mathcal{H}_1 \oplus \mathcal{H}_2, \quad (5)$$

where \mathcal{H}_S denotes the local Hilbert space of a spin- S . The pseudo-spin operators are defined as

$$\hat{S}_{-,k} = b_k = \hat{S}_{+,k}^+, \quad (6a)$$

$$\hat{S}_{z,k} = \frac{n_k}{2} - 1, \quad (6b)$$

$$\hat{S}_k^2 = \left(\frac{n_k}{2} - 1 \right)^2 + \frac{b_k^+ b_k + b_k b_k^+}{2}, \quad (6c)$$

where $n_k = \sum_\sigma (n_{k\sigma} + n_{-k\sigma})$ is the operator counting the total number of particles in the modes k and $-k$ and

$$b_k = c_{-k\downarrow} c_{k\uparrow} + c_{k\downarrow} c_{-k\uparrow} \quad (7)$$

is the operator annihilating a Cooper-pair. By analyzing the Hamiltonian in a given $k > 0$ mode, the lowest energy is found in the three-dimensional pseudo-spin triplet subspace spanned by

$$|0_k\rangle = |0, 0, 0, 0\rangle, \quad (8a)$$

$$|S_k\rangle = \frac{1}{\sqrt{2}} b_k^+ |0_k\rangle = \frac{1}{\sqrt{2}} (|\uparrow_k, \downarrow_{-k}, 0, 0\rangle + |0, 0, \uparrow_{-k}, \downarrow_k\rangle), \quad (8b)$$

$$|D_k\rangle = |\uparrow_k, \downarrow_{-k}, \uparrow_{-k}, \downarrow_k\rangle = \frac{1}{\sqrt{2}} b_k^+ |S_k\rangle \quad (8c)$$

which, from the point of view of the physical spin, are singlet states. Eqs. (8) represents the many-body bases compared to the conventional BCS case, wherein the respective states contain 0, 2 and 4 particles. From now on, we will consider only half of the first Brillouin zone instead of all k modes and use the notation $k > 0$ for the half Brillouin zone independently from the actual dimension of the system. The number of $k > 0$ modes is $N/2$. On the subspace of the states in Eq. (8), the grand canonical Hamiltonian $H_{MF} - \mu\hat{N}$ is represented by

$$\mathbf{H}_k = \begin{bmatrix} 0 & -\sqrt{2}\Delta^* & 0 \\ -\sqrt{2}\Delta & 2\varepsilon(k) - 2\mu & -\sqrt{2}\Delta^* \\ 0 & -\sqrt{2}\Delta & 4\varepsilon(k) - 4\mu + 2U \end{bmatrix} \quad (9)$$

where we assumed that $\varepsilon(k) = \varepsilon(-k)$. The effective Hamiltonian in Eq. (9) is in accordance with Ref. [15]. Eq. (9) can in principle be diagonalized, but its eigenvalues are only simple expressions in the uncorrelated,

$U = 0$ case as $2(\varepsilon(k) - \mu) + 2s\sqrt{(\varepsilon(k) - \mu)^2 + |\Delta|^2}$ with $s = -1, 0$ and 1 . We finally mention that the non-Fermi liquid non-superconducting ground state of the HK model has huge degeneracy[12], but the extra pairing interaction g lifts this ground state degeneracy and results in a non-degenerate superconducting ground state.

Within mean-field approximation, the ground state phase diagram at half-filling is sketched in Fig. 1. When the two Hubbard bands overlap, $U < W$, the superconducting phase is favoured for any finite pairing interaction g . In the following section, we study the dynamics following a sudden quench of the HK interaction U inside this regime by keeping g fixed, unchanged. This means that we change the non-Fermi liquid properties of the non-interacting system by quenching U and ask, how this affects the already existing superconducting properties. Non-equilibrium dynamics of the non-superconducting HK model was also investigated[26] for the photoemission spectra.

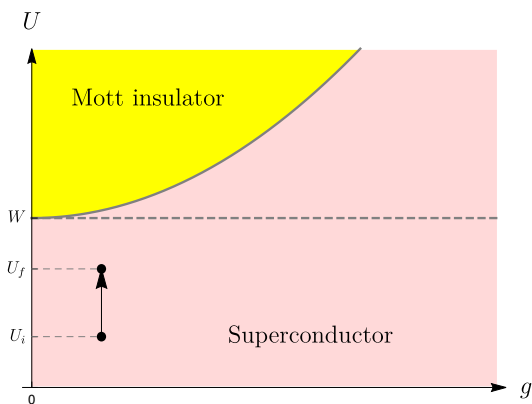


FIG. 1. Schematic of the mean-field phase diagram at $T = 0$ and at half-filling. In the absence of superconductivity ($g = 0$), the system forms a non-Fermi liquid for $U < W$. The arrow indicates the sudden quench of the interaction strength studied in Sec. III.

III. SUDDEN QUENCH OF THE INTERACTION STRENGTH

The system is initially prepared in the ground state corresponding to a pairing interaction g and initial U_i in the equilibrium non-Fermi liquid phase. As shown in the previous section, the ground state is a singlet state corresponding to the total spin zero. At $t = 0$, the strength of U is changed from U_i to U_f within the non-Fermi liquid region, namely $0 < U_{i,f} < W$. The resulting Hamiltonian conserves the total and the pseudospin as well and, hence, the dynamics will not be driven out of the pseudospin triplet subspace, spanned by Eq. (8).

The most general form of the singlet wavefunction can

be written in the form of

$$|\Psi(t)\rangle = \prod_{k>0} (x_k(t)|0_k\rangle + y_k(t)|S_k\rangle + z_k(t)|D_k\rangle) \quad (10)$$

where the coefficients fulfill $|x_k(t)|^2 + |y_k(t)|^2 + |z_k(t)|^2 = 1$ at any time instants. The conventional uncorrelated, $U = 0$ BCS theory follows from $x_k(t) = u_k^2(t)$, $y_k(t) = \sqrt{2}u_k(t)v_k(t)$ and $z_k(t) = v_k^2(t)$ with $u_k(t)$ and $v_k(t)$ the conventional Bogoliubov coefficients[27], satisfying $|u_k(t)|^2 + |v_k(t)|^2 = 1$. The dynamics is governed by the Hamiltonian in Eq. (9), resulting in the dynamical equations for the wavefunction coefficients as

$$i\partial_t\psi(t) = \mathbf{H}_k\psi(t) \quad (11)$$

where $\psi(t) = [x_k(t), y_k(t), z_k(t)]^T$ and we used U_f in \mathbf{H}_k together with $\mu = U_f/2$, corresponding to half filling. The quench in the interaction strength also involves a quench in the chemical potential in order to not change the filling of the system. Note that in Eq. (11), the gap is time-dependent. Within the realm of self-consistent mean-field theory, the gap is calculated based on the instantaneous coefficients as

$$\Delta(t) = \frac{g}{N} \sum_{k>0} \sqrt{2} (x_k^*(t)y_k(t) + y_k(t)^*z_k(t)) \quad (12)$$

which is an extension of the calculation presented in Refs. [5, 21, 28] to the HK model. The initial condition for Eq. (11) is determined by the lowest energy eigenvectors of Eq. (9) when the interaction strength is set to U_i and $\mu = U_i/2$ from Eq. (2).

Since the Hamiltonian does not commute with the number of particles, it is also a question if the filling factor remains $1/2$. It can, however, be shown that the expectation value of the number of particles is expressed as

$$N_e(t) = \sum_{k>0} (2|y_k|^2 + 4|z_k|^2) \quad (13)$$

and its time derivative is zero under the dynamics governed by Eq. (11), i.e., the half-filling is preserved.

IV. ORDER PARAMETER DYNAMICS AND PHASE DIAGRAM

The differential equations in Eq. (11) cannot be solved analytically. Here we have three coupled differential equations compared to the conventional case involving only two [5, 11]. However, the main difficulty stems from the self-consistency relation from Eq. (12) which introduces a highly non-linear coupling between the dynamical variables. Moreover, even the eigenvalue problem in Eq. (9) does not admit a simple, transparent analytical solution for nonzero U . The dynamical equations are solved numerically using the explicit Runge-Kutta method of order 8(5,3) for $x_k(t)$, $y_k(t)$ and

$z_k(t)$. We assume that all quantities depend on k only through $\varepsilon(k)$, therefore $\sum_k f(\varepsilon(k)) = N \int_{-W/2}^{W/2} \frac{d\varepsilon}{W} f(\varepsilon)$ with $f(\varepsilon(k))$ corresponding to some physical quantity as in e.g. Eq. (13), $1/W$ is the density of states. The total energy range $[-W/2; W/2]$ is discretized with the resolution $N_{res} = 8000$, i.e. we consider N_{res} equidistant energy values within the total energy range. Other band structures with bounded density of states are not expected to yield qualitatively different results. The order parameter is computed based on Eq. (12), and the typical time evolutions exhibit three typical behaviors, see Fig. 2 (a). When the difference between the initial and final interaction strength is small, the gap exhibits undamped, persistent oscillations around a finite value after a transient phase, see for example the quench corresponding to $U_i = 0.45W$.

When the difference is intermediate, the gap converges to a finite value through damped oscillations, see for example the quench corresponding to $U_i = 0.4W$ or $U_i = 0.35W$. The third kind of behavior is observed when the difference between the initial and final interaction strengths is large. In this case, see for example the quench from $U_i = 0.3W$, the order parameter converges to zero in an oscillating fashion with exponential time dependence as $\Delta(t) \sim \exp(-\lambda t)$, where λ is the Landau damping.

All of these temporal behaviors have also been witnessed after quenching the pairing interaction in regular BCS superconductors [5]. However, there are important differences compared to the conventional BCS case. Undamped oscillations are observed if the final equilibrium gap is much larger than the initial one, while decaying order parameter is found in the opposite regime, i.e., when the final equilibrium gap is much smaller. Further difference is that in the BCS case, the time evolution is determined only by the ratio Δ_i/Δ_f , while in the HK model, more energy scales are present including e.g. $U_{i,f}$, which all influence the characteristics of the time evolution.

It is also interesting to note that the frequency of the oscillations in the order parameter is not solely determined by the final gap, Δ_f , but it is influenced by the numerous energy scales including those of the initial state. In Fig. 2 (a), for example, the final Hamiltonian is the same for all quenches and the only difference is in the initial state but the curves exhibit oscillations with different frequencies.

The cases, when the order parameter decays to zero, can be regarded as dynamical phase transition (DPT) [29, 30]. To detect DPT numerically, we evaluate the average gap as

$$\bar{\Delta} = \frac{1}{N_{t_{\text{cutoff}}}} \sum_{t_i > t_{\text{cutoff}}} \Delta(t_i) \quad (14)$$

where we introduced the temporal cut-off t_{cutoff} to avoid effects from the transient period. In the above expression, $N_{t_{\text{cutoff}}}$ is the number of discrete time instants fulfilling $t_i > t_{\text{cutoff}}$. In this way, $\bar{\Delta}$ describes the long term aver-

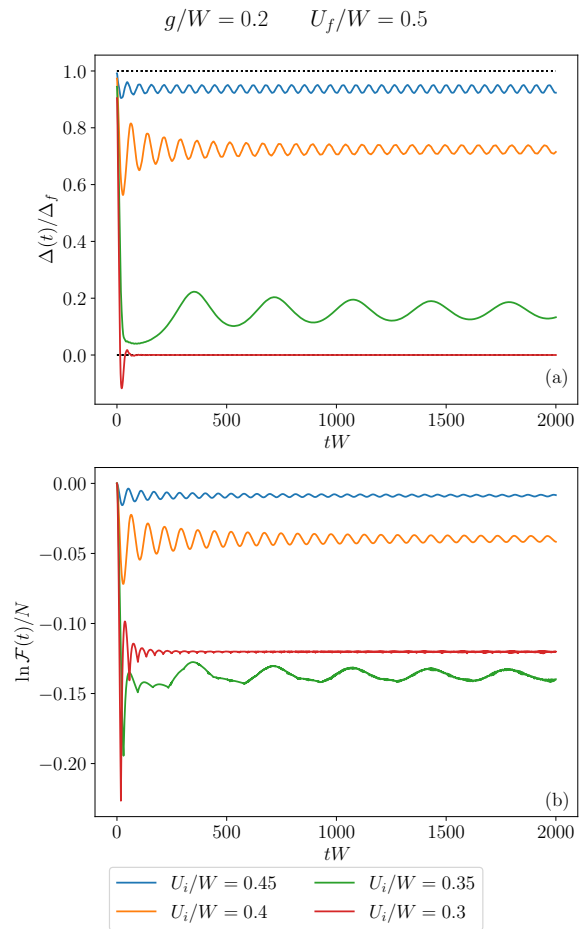


FIG. 2. Time evolution of the order parameter, $\Delta(t)$, and the Loschmidt echo, $\mathcal{F}(t)$ for various initial interaction strength, U_i . The green curve corresponding to $U_i/W = 0.35$ denotes a non-zero late time superconducting order parameter, yet non-analytic structures are already present in the Loschmidt echo.

age of the order parameter. For the DPT case, i.e., when the gap decays to zero, the time average is approximately zero. The average order parameter as a function of U_i is represented by the solid line in Fig. 3 for $g/W = 0.2$ and $U_f/W = 0.5$. At the DPT, $\bar{\Delta} = 0$ and a sharp transition is detected at $U_i/W \approx 0.34$ and $U_i/W \approx 0.66$.

We further analyze the characteristics of the oscillations when the gap remains finite, i.e., in the absence of DPT. By extracting the local maxima and minima of the oscillations, we observe a power law decay with exponent close to $-1/2$ of the amplitudes, in accord with the result of Ref. 24. By fitting $\Delta_{\min/\max} + A_{\min/\max} t^{-1/2}$ separately to the local minima and maxima, we compute the long term $\Delta_{\min/\max}$ values of the gap which are also plot in Fig. 3. For comparison, we also show the HK interaction dependence of the initial superconducting order parameter. It can be observed that $\Delta_{\min/\max}$ coincide with Δ_f if $U_i = U_f$, i.e. no oscillations are present. As U_i moves away from U_f , we first find persistent oscillations.

This behavior then transforms smoothly to damped oscillations. For large quenches, we find an exponential damping of the order parameter as $\Delta(t) \sim \exp(-\lambda t)$ with λ the Landau damping. Its value is extracted from the time evolution and is also plotted in Fig. 3. While this phase diagram is not universal, namely the specific values depend on the chosen initial and final values of the interactions, we expect qualitatively similar features for other values g and U_f , see Appendix.

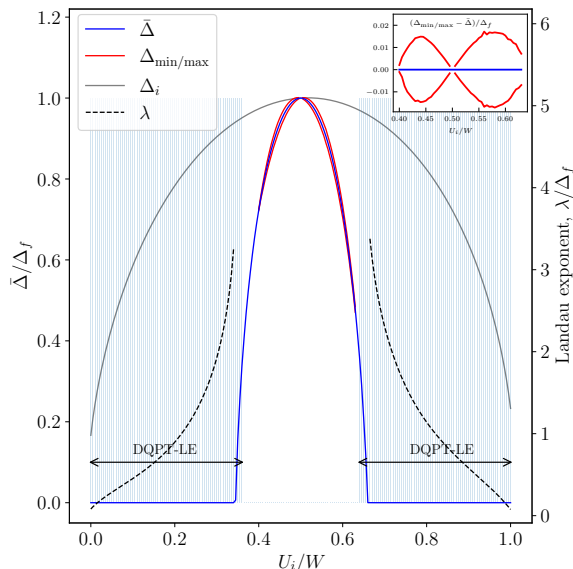


FIG. 3. The average order parameter (solid, blue line) for $U_f/W = 0.5$ as a function of initial interaction strength U_i measured on the left vertical axis, together with its maximal and minimal value in the case of persistent oscillation. We also plot the equilibrium order parameter of the initial state (solid, gray line) for comparison, in accord with Refs. [12, 14, 15]. The right vertical axis shows the Landau damping parameter (dashed, black lines) in the region when the order parameter vanishes in the long time limit. The hatching indicates the regime where the Loschmidt echo exhibits non-analytic features. It does not match the region of vanishing order parameter, the non-analyticities already appear in the region when the long time limit of the superconducting order parameter approaches a non-zero constant. For the plot, only the time instants after $t_{\text{cutoff}} = 300/W$ were taken into account. The inset zooms into the region of persistent oscillation for small quenches.

We note that in Ref. [5] the dynamical equations were written for the pseudospin components instead of x_k , y_k and z_k . We choose to use these coefficients because they also enable to calculate other quantities such as the Loschmidt echo.

V. LOSCHMIDT ECHO

Another definition of the dynamical quantum phase transition (DQPT) involves the time dependent non-

analytic feature in the Loschmidt echo [8, 11, 31, 32]. To this end, we study the overlap between the time-evolved and the initial state, $\mathcal{F}(t) = |\langle \Psi_0 | \Psi(t) \rangle|^2$, where the time evolution involves the grand canonical Hamiltonian from Eq. (9). By using the coefficients x_k , y_k and z_k from the wavefunction, the Loschmidt echo is expressed as

$$\mathcal{F}(t) = \prod_{k>0} |x_k(0)^* x_k(t) + y_k(0)^* y_k(t) + z_k(0)^* z_k(t)|^2 \quad (15)$$

which can be computed directly from the numerical solution of the differential equations in Eq. (11). For a conventional BCS non-equilibrium dynamics[11], this can be expressed in terms of the pseudospin expectation values from Eq. (6), which does not work in our case when the non-superconducting ground state realizes a non-Fermi liquid. In our case, the chemical potential is included in the Hamiltonian in Eq. (9) describing the dynamics of the system, and the ensuing time dependent overlap is the grand canonical Loschmidt echo[11] using Eq. (2) as well. The time-dependence of the Loschmidt echo is plotted in Fig. 2 (b). It exhibits non-analytical behaviour when the difference is large between the initial and final HK interaction strength. It is important to note that the time instants of the non-analyticity do not coincide with the critical times of the order parameter similarly to Ref. [33].

To study the non-analyticities systematically, we define from the numerical values $f_i = \ln(\mathcal{F}(t_i)) / N$ the discrete second derivative

$$s_i = \frac{f_{i-1} - 2f_i + f_{i+1}}{\Delta\tau^2} \quad (16)$$

where $\Delta\tau$ is the time step in the numerical simulation. As a continuous function, the Loschmidt echo would show non-analyticities as diverging second derivatives. Numerically, we claim that the Loschmidt echo is non-analytic if there exists i such that both $|s_i| > 2(|s_{i-1}| + |s_{i+1}|)$ and $|s_i| > 0.1\Delta\tau$ is fulfilled. In Fig. 3, the hatching indicates the region where non-analytic behavior was found, i.e., where DQPT emerges. For the specific example of $g/W = 0.2$ and $U_f/W = 0.5$, the transition between non-analytic and analytic regimes is found at $U_i/W \approx 0.36$ and $U_i/W \approx 0.64$. Interestingly, these critical values slightly differ from those of the DPT indicated by the order parameter. In particular, the green curve of Fig. 2 corresponding to $U_i/W = 0.35$ highlights clearly what we discussed above: while the order parameter approaches a constant, non-zero value in the long time limit, hence no DPT occurs, the Loschmidt echo displays non-analytic behaviour, indicating the occurrence of DQPT.

VI. MOMENTUM SPACE ENTANGLEMENT

In order to better understand and characterize the properties of the steady state, we focus on its entangle-

ment properties[34–36]. While the most common partitioning for entanglement is spatial, i.e. done in real-space, other ways of partitioning are equally fruitful[37]. Cooper pairs are made of particles with opposite momentum therefore characterizing their entanglement properties in momentum space is expected to contain all essential information about the non-local quantum correlations and superconductivity. This is defined as

$$S(t) = -\text{Tr}[\rho_+(t) \ln \rho_+(t)] \quad (17)$$

where $\rho_+(t) = \text{Tr}_- [|\Psi(t)\rangle\langle\Psi(t)|]$ is the reduced density matrix for $k > 0$ after tracing out the $k < 0$ modes. By using the coefficients of the wavefunction, the momentum space entanglement entropy is

$$S(t) = -\sum_{k>0} \left(|x_k(t)|^2 \ln |x_k(t)|^2 + |y_k(t)|^2 \ln \left(\frac{|y_k(t)|^2}{2} \right) + |z_k(t)|^2 \ln |z_k(t)|^2 \right). \quad (18)$$

The entanglement is computed based on the numerical solutions for x_k , y_k and z_k and is shown in Fig. 4. Here, S_i corresponds to the initial state entanglement, while \bar{S} stands for the late time average of the entanglement entropy.

The momentum space entanglement entropy satisfies a volume law even for the ground state. We find that this entanglement does not change significantly between the initial and final state, though small enhancement or suppression is observed depending on the initial and final HK interaction. The most notable feature is that this entanglement is large for large initial U_i when the late time superconducting order parameter vanishes. Even though superconductivity is absent from this steady state, the entanglement between modes with positive and negative momenta is very large for large initial HK interaction. The derivative of the entanglement with respect to the change of the HK interaction, i.e. $\frac{d\bar{S}}{d(U_i - U_f)}$ (which is $\frac{d\bar{S}}{dU_i}$ for the current protocol) displays sharp peaks when DPT happens. That is, it signals the late time vanishing of superconductivity.

VII. CONCLUSION

In this paper, we studied the time evolution following a sudden quench of the interaction HK interaction U in the superconducting HK model by leaving the superconducting coupling intact. The time evolution of the order parameter exhibits three distinct behaviours depending on the value of the initial and final value of the interaction, U_i and U_f . We find that for small (intermediate) quenches, the superconducting gap exhibits undamped

(damped) oscillation around a finite value while for larger quenches, the gap converges to zero in an oscillating fashion. The latter is regarded as one type of DPT.

In addition, we also inspected the time dependence of the Loschmidt echo, corresponding to the overlap of

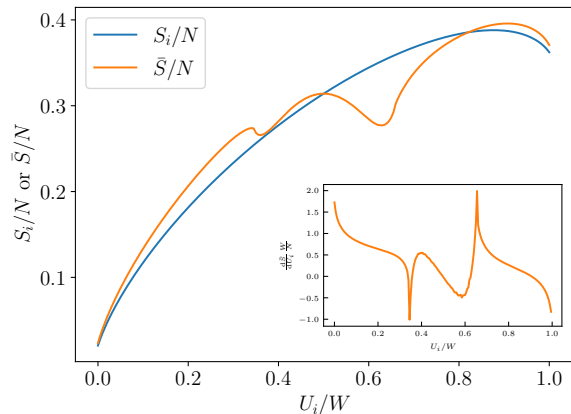


FIG. 4. The average momentum space entanglement entropy for $U_f/W = 0.5$ between $k > 0$ and $k < 0$ modes is plotted for the initial state as well as in the steady state. The inset depicts the interaction derivative of the entropy in the steady state, displaying sharp peaks at the DPT points.

the initial and time evolved wavefunctions. Non-analytic temporal behaviour is identified for large quenches, though the "phase boundary" for this to happen does not coincide exactly to what is identified from the long time dynamics of the order parameter. Therefore, DPTs and DQPTs do not coincide.

By investigating the momentum space entanglement between positive and negative energy modes, responsible for superconductivity, we find that this entanglement remains very large even for regions with vanishing superconducting order parameter, corresponding to large initial value of the HK interaction. The derivative of the momentum space entanglement with respect to HK interaction in the steady state clearly signals the vanishing amplitude of the superconducting gap by developing sharp peaks at the critical value of HK interaction, corresponding to DPT.

ACKNOWLEDGMENTS

We acknowledge the support of the National Research, Development and Innovation Office - NKFIH Project Nos. K134437 and K142179. Á.B. acknowledges the support of the Slovenian Research and Innovation Agency (ARIS) under P1-0416 and J1-3008.

[1] J. Dziarmaga, *Dynamics of a quantum phase transition and relaxation to a steady state*, Adv. Phys. **59**, 1063

(2010).

- [2] A. Polkovnikov, K. Sengupta, A. Silva, and M. Vengalattore, *Colloquium : Nonequilibrium dynamics of closed interacting quantum systems*, Rev. Mod. Phys. **83**, 863 (2011).
- [3] A. Mitra, *Quantum quench dynamics*, Annual Review of Condensed Matter Physics **9**(Volume 9, 2018), 245 (2018).
- [4] M. S. Foster, V. Gurarie, M. Dzero, and E. A. Yuzbashyan, *Quench-induced floquet topological p-wave superfluids*, Phys. Rev. Lett. **113**, 076403 (2014).
- [5] R. A. Barankov and L. S. Levitov, *Synchronization in the bcs pairing dynamics as a critical phenomenon*, Phys. Rev. Lett. **96**, 230403 (2006).
- [6] D. J. Young, A. Chu, E. Y. Song, D. Barberena, D. Wellnitz, Z. Niu, V. M. Schafer, R. J. Lewis-Swan, A. M. Rey, and J. K. Thompson, *Observing dynamical phases of bcs superconductors in a cavity qed simulator*, Nature **625**, 679 (2024).
- [7] J. Marino, M. Eckstein, M. S. Foster, and A. M. Rey, *Dynamical phase transitions in the collisionless pre-thermal states of isolated quantum systems: theory and experiments*, Reports on Progress in Physics **85**(11), 116001 (2022).
- [8] M. Heyl, *Dynamical quantum phase transitions: a review*, Reports on Progress in Physics **81**(5), 054001 (2018).
- [9] M. Heyl, A. Polkovnikov, and S. Kehrein, *Dynamical quantum phase transitions in the transverse-field ising model*, Phys. Rev. Lett. **110**, 135704 (2013).
- [10] F. Pollmann, S. Mukerjee, A. G. Green, and J. E. Moore, *Dynamics after a sweep through a quantum critical point*, Phys. Rev. E **81**, 020101 (2010).
- [11] C. Rylands, E. A. Yuzbashyan, V. Gurarie, A. Zabalo, and V. Galitski, *Loschmidt echo of far-from-equilibrium fermionic superfluids*, Annals of Physics **435**, 168554 (2021), special issue on Philip W. Anderson.
- [12] P. W. Phillips, L. Yeo, and E. W. Huang, *Exact theory for superconductivity in a doped mott insulator*, Nature Physics **16**(12), 1175 (2020).
- [13] J. Zaanen, *Carriers that count*, Nat. Phys. **16**, 1171 (2020).
- [14] Y. Li, V. Mishra, Y. Zhou, and F.-C. Zhang, *Two-stage superconductivity in the hatsugai-kohmoto-bcs model*, New Journal of Physics **24**(10), 103019 (2022).
- [15] H.-S. Zhu and Q. Han, *Effects of electron correlation on superconductivity in the hatsugai-kohmoto model**, Chinese Physics B **30**(10), 107401 (2021).
- [16] H.-S. Zhu, Z. Li, Q. Han, and Z. D. Wang, *Topological s-wave superconductors driven by electron correlation*, Phys. Rev. B **103**, 024514 (2021).
- [17] J. Zhao, L. Yeo, E. W. Huang, and P. W. Phillips, *Thermodynamics of an exactly solvable model for superconductivity in a doped mott insulator*, Phys. Rev. B **105**, 184509 (2022).
- [18] Z. Sun and H.-Q. Lin, *Emergence of a diverse array of phases in an exactly solvable model*, Phys. Rev. B **109**, 115108 (2024).
- [19] Y. Hatsugai and M. Kohmoto, *Exactly solvable model of correlated lattice electrons in any dimensions*, Journal of the Physical Society of Japan **61**(6), 2056 (1992).
- [20] D. Lidsky, J. Shiraishi, Y. Hatsugai, and M. Kohmoto, *Simple exactly solvable models of non-fermi-liquids*, Phys. Rev. B **57**, 1340 (1998).
- [21] R. A. Barankov, L. S. Levitov, and B. Z. Spivak, *Collective rabi oscillations and solitons in a time-dependent bcs pairing problem*, Phys. Rev. Lett. **93**, 160401 (2004).
- [22] V. Gurarie, *Nonequilibrium dynamics of weakly and strongly paired superconductors*, Phys. Rev. Lett. **103**, 075301 (2009).
- [23] E. A. Yuzbashyan and M. Dzero, *Dynamical vanishing of the order parameter in a fermionic condensate*, Phys. Rev. Lett. **96**, 230404 (2006).
- [24] A. F. Volkov and S. M. Kogan, *Collisionless relaxation of the energy gap in superconductors*, JETP **38**, 1018 (1974).
- [25] P. W. Anderson, *Random-phase approximation in the theory of superconductivity*, Phys. Rev. **112**, 1900 (1958).
- [26] R. D. Nesselrodt and J. K. Freericks, *Exact solution of two simple non-equilibrium electron-phonon and electron-electron coupled systems: The atomic limit of the holstein-hubbard model and the generalized hatsugai-kohmoto model*, Phys. Rev. B **104**, 155104 (2021).
- [27] M. Tinkham, *Introduction to Superconductivity* (MacGraw-Hill, New York, 1996).
- [28] F. Peronaci, M. Schiró, and M. Capone, *Transient dynamics of d-wave superconductors after a sudden excitation*, Phys. Rev. Lett. **115**, 257001 (2015).
- [29] B. Zunkovic, M. Heyl, M. Knap, and A. Silva, *Dynamical quantum phase transitions in spin chains with long-range interactions: Merging different concepts of nonequilibrium criticality*, Phys. Rev. Lett. **120**, 130601 (2018).
- [30] A. Leroise, B. Žunkovič, J. Marino, A. Gambassi, and A. Silva, *Impact of nonequilibrium fluctuations on prethermal dynamical phase transitions in long-range interacting spin chains*, Phys. Rev. B **99**, 045128 (2019).
- [31] F. Andraschko and J. Sirker, *Dynamical quantum phase transitions and the loschmidt echo: A transfer matrix approach*, Phys. Rev. B **89**, 125120 (2014).
- [32] C. Karrasch and D. Schuricht, *Dynamical phase transitions after quenches in nonintegrable models*, Phys. Rev. B **87**, 195104 (2013).
- [33] S. Vajna and B. Dóra, *Disentangling dynamical phase transitions from equilibrium phase transitions*, Phys. Rev. B **89**, 161105 (2014).
- [34] J. Eisert, M. Cramer, and M. B. Plenio, *Colloquium : Area laws for the entanglement entropy*, Rev. Mod. Phys. **82**, 277 (2010).
- [35] M. Nielsen and I. Chuang, *Quantum Computation and Quantum Information* (Cambridge University Press, Cambridge, 2000).
- [36] L. Amico, R. Fazio, A. Osterloh, and V. Vedral, *Entanglement in many-body systems*, Rev. Mod. Phys. **80**, 517 (2008).
- [37] R. Thomale, D. P. Arovas, and B. A. Bernevig, *Nonlocal order in gapless systems: Entanglement spectrum in spin chains*, Phys. Rev. Lett. **105**, 116805 (2010).

Appendix A: HK quench with final interaction strength $U_f/W = 0.3$

To demonstrate qualitatively similar dynamical features of the HK model with different final interaction strength, we perform numerical calculations for $U_f/W = 0.3$. The typical time evolution of the order parameter is plotted in Fig. 5 The results displays again the three distinct behaviors, namely the persistent oscilla-

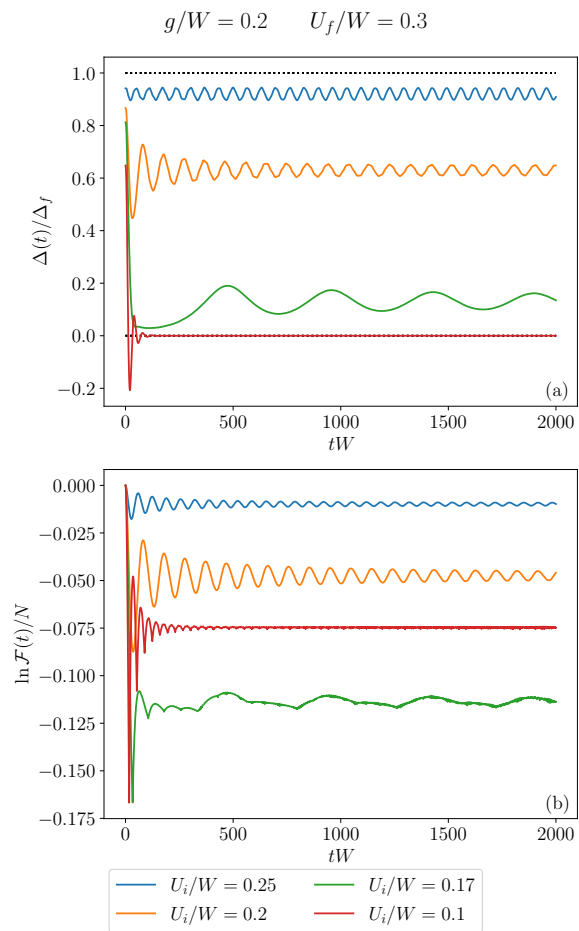


FIG. 5. Time evolution of the order parameter, $\Delta(t)$, and the Loschmidt echo, $\mathcal{F}(t)$ for various initial interaction strength, U_i and for $U_f/W = 0.3$.

tion, the damped oscillation and the vanishing behavior. By sweeping the initial HK interaction between zero and W , we obtain the phase diagram as shown in Fig. 6, which exhibits qualitatively similar features to the case of $U_f/W = 0.5$. The only difference is in the location of the different regions. Finally, we compute the momentum space entanglement based on Eq. (18) of the main text. The time evolution of the entanglement is shown in Fig. 7. We also study the initial and the steady state entanglement as a function the initial HK interaction, see Fig. 8, and find similar features as for $U_f/W = 0.5$.

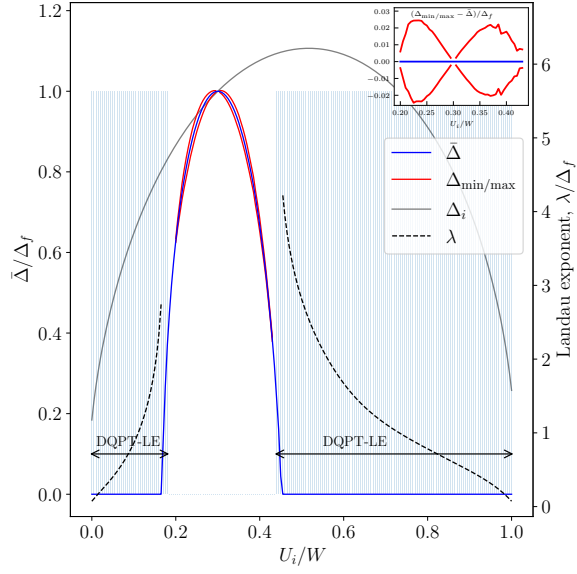


FIG. 6. The average order parameter (solid, blue line) for $U_f/W = 0.3$ as a function of initial interaction strength U_i measured on the left vertical axis, together with its maximal and minimal value in the case of persistent oscillation. The right vertical shows Landau damping parameter (dashed, gray line) in the region when the order parameter vanishes in the long time limit. The hatching indicates the regime where the Loschmidt echo exhibits non-analytic features. For the plot, only the time instants after $t_{\text{cutoff}} = 300/W$ were taken into account. The inset zooms into the region of persistent oscillation for small quenches.

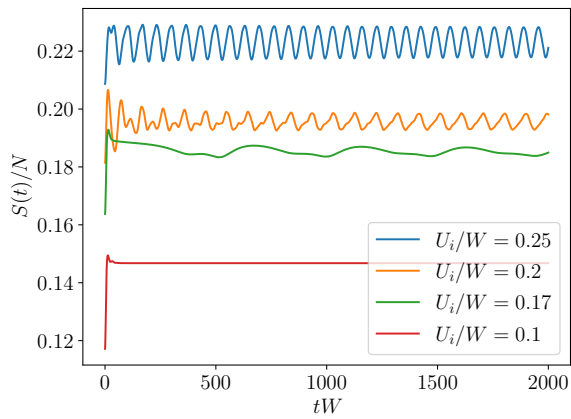


FIG. 7. Time evolution of the momentum space entanglement for various values of the initial HK interaction and for the final interaction strength $U_f/W = 0.3$.

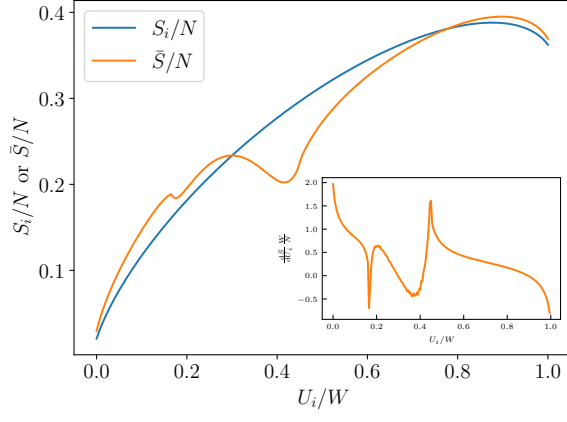


FIG. 8. The average momentum space entanglement entropy for $U_f/W = 0.3$ between $k > 0$ and $k < 0$ modes is plotted for the initial state as well as in the steady state. The inset shows the interaction derivative of the steady state entropy.